LOW-COST, HIGH RESOLUTION X-BAND LABORATORY RADAR SYSTEM FOR SYNTHETIC APERTURE RADAR APPLICATIONS

Gregory L. Charvat, MSEE
Department of Electrical and Computer Engineering
Michigan State University
2120 Engineering Building
East Lansing, MI 48825

ABSTRACT

Using a discarded garage door opener, an old cordless drill, and a collection of surplus microwave parts, a high resolution X-band linear rail synthetic aperture radar (SAR) imaging system was developed for approximately $240 material cost. Entry into the field of radar cross section measurements or SAR algorithm development is often difficult due to the cost of high-end precision pulsed IF or other precision radar test instruments. The low cost system presented in this paper is a frequency modulated continuous wave radar utilizing a homodyne radar architecture. Transmit chirp covers 8 GHz to 12.4 GHz with 15 dBm of transmit power. Due to the fairly wide transmit bandwidth of 4.4 GHz, this radar is capable of approximately 1.4 inches of range resolution. The dynamic range of this system was measured to be 60 dB thus providing high sensitivity. The radar system traverses a 96 inch automated linear rail, acquiring range profiles at any user defined spacing. SAR imaging results prove that this system could easily image objects as small as pushpins and 4.37 mm diameter steel spheres.

Keywords: Radar Imaging, Synthetic Aperture Radar, Measurement Systems, Low Cost Radar, Low Cost Rail SAR.

1. Introduction

A low cost, high resolution, X-band synthetic aperture radar (SAR) imaging system was developed by the Michigan State University Electromagnetics Research Group. The purpose behind this research effort was to develop a low cost entry level system for use by universities or small businesses looking to enter the field of radar cross section (RCS) measurements or SAR algorithm development. A high performance but low cost rail SAR was developed using a discarded garage door opener, an old cordless drill, and some surplus microwave parts for a very low total material cost. In this paper the implementation, range profile data results, and radar imagery from this system will be presented.

A background discussion on frequency modulated continuous wave (FMCW) radar is presented in section 2. An explanation of the radar system design is presented in section 3. Section 4 presents range profile measurement results. High resolution SAR imaging results are presented in section 5. Section 6 will discuss conclusions and future work. References are provided in section 7.

2. Background

FMCW radar was first widely used in radio altimeters, starting in the mid 1930's [1]. FMCW has a number of design advantages, including a high average power and short range capabilities. FMCW is unique in its ability to range targets extremely close to the radar transmit and receive antennas. The major disadvantage of FMCW radar (or any CW radar system) is antenna coupling. The transmit to receive antenna coupling limits dynamic range in a FMCW radar system.

When a CW radar system is FM modulated, the range to target information provided is in the form of beat frequencies. This is known as FMCW radar. The beat frequencies on the video output of an FMCW radar system correspond to multiple targets and their corresponding ranges. FMCW radar systems are also capable of measuring the Doppler shift of a moving target. The block diagram of a basic FMCW radar system is shown in figure 1.

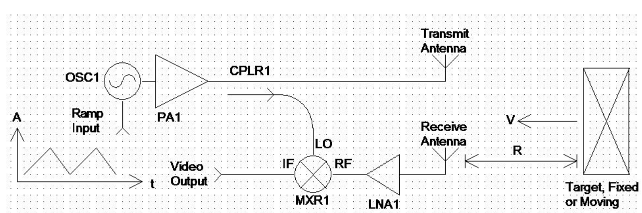

Figure 1: Block diagram of a basic FMCW radar system.

Looking at figure 1, OSC1 is FM modulated with a triangular ramp input with a period of 2 ms. The triangular ramp is an alternating linear ramp with both positive and negative slopes as shown in figure 2.

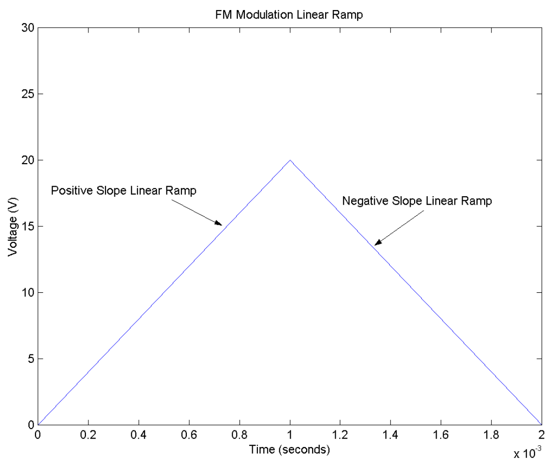

Figure 2: Linear ramp used to FM modulate the FMCW radar system.

The FM output of OSC1 is fed into PA1. PA1 amplifies OSC1 to an appropriate transmit level. The output of OSC1 is radiated out of the transmit antenna. The FM modulated carrier is reflected off of the target at a range of R meters. The reflected signal is delayed in time on its way to and from the target. The reflected signal is received by the receive antenna, and amplified by LNA1. The output of LNA1 is fed into the RF port of MXR1. Some power from PA1 is coupled into the LO port of MXR1. When the LO and the RF are multiplied together in MXR1, the IF output of MXR1 is the range to target in frequency. This range to target in terms of frequency is known as the beat frequency. The greater the beat frequency on the IF output port of MXR1, the greater the range to target. If the target is moving, then the Doppler shift of the moving target is added onto the beat frequency present on the IF port of MXR1. The relationship between frequency, FM chirp bandwidth, range to target, and Doppler frequency shift can be found using the equations for both a positive and a negative linear ramp modulation waveform [2]. When a positively sloped linear ramp FM modulates OSC1, the beat frequency at the IF port of MXR1 is represented by:

$$f_b = f_b^+ = \frac{8\Delta f f_m R}{c} - f_d \tag{1}$$

Where: f_b = the beat frequency at the IF port of MXR1

f_b^+ = the beat frequency at the IF port of MXR1 when OSC1 is modulated with a positive linear ramp.

Δf = chirp frequency deviation

f_m = FM modulation rate

R = range to target

When a negatively sloped linear ramp FM modulates OSC1, the beat frequency at the IF port of MXR1 is represented by:

$$f_b = f_b^- = \frac{8\Delta f f_m R}{c} + f_d \tag{2}$$

Where: f_b^- = the beat frequency at the IF port of MXR1 when OSC1 is modulated with a negative linear ramp

From the equations above, the range to target is found using:

$$R = \frac{c}{8\Delta f f_m}\langle f_b \rangle \tag{3}$$

Where: $\langle f_b \rangle$ = the average frequency difference

If the target is moving, the velocity of the target can be found using:

$$v = \frac{\lambda}{4}\left(f_b^- - f_b^+\right) \tag{4}$$

The amplitude of the return signals can be approximated using the radar range equation [2].

The most important concept explained here is that a shift in time corresponds to a shift in frequency. This is because the radar is frequency modulated in time. The current value of the transmitted frequency is different than what was transmitted 2 ns ago. These small and subtle frequency differences make up the beat frequencies on the IF output of MXR1, and hence the range to target information in the form of low frequency beats.

The Electromagnetics Group at Michigan State University has previously presented a low cost FMCW rail SAR imaging system, known as the unique approach to FMCW [3, 4]. This system was capable of SAR imaging, however it lacked the sensitivity and range resolution required to research highly advanced SAR imaging algorithms, and for that reason it was decided to develop a more sophisticated high resolution FMCW radar system [5]. Based on promising results from [5] it was then decided to utilize this system as a high resolution linear rail SAR imaging system.

3. System Implementation

The low cost high resolution X-band laboratory radar system discussed in this paper is a homodyne FMCW system like that shown in section 2. The radar system front end is shown in Figure 3. Figure 4 shows the data acquisition, power supply, and motion control chassis. Figure 5 shows the complete system in operation.

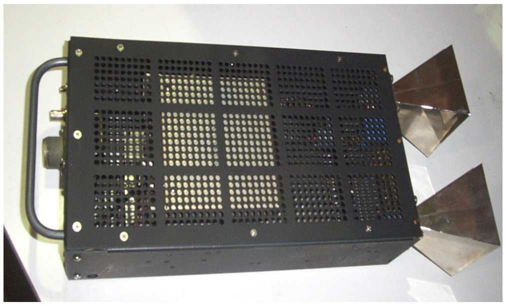

Figure 3: The low cost high resolution X-band laboratory radar system front end.

Figure 4: Data acquisition, power supply, and motion control chassis.

Figure 5: Compete system in operation.

This particular radar system chirps linearly from 8 GHz to 12.4 GHz with a chirp rate of 440 GHz/sec. The sensitivity of this system is 25.1 µV, and the dynamic range is 60 dB. A block diagram of the system is shown in Figure 6.

OSC1 is a voltage tuned YIG oscillator that tunes from 8 GHz to 12.4 GHz. OSC1 is modulated by a linear ramp generated by DAC1 and OP3, thus producing the 8 GHz to 12.4 GHz transmit chirp. The output of OSC1 feeds into the directional coupler CLPR1. The coupled output of CLPR1 is fed through circulator Circ2 and feeds the LO port of the double balanced mixer MXR1. The through port of CLPR1 is fed through the circulator Circ1 to the transmit horn antenna Ant1. Ant1 is a standard gain X-band horn that is fed by a WR90 waveguide transition. The transmit power of the chirp signal is 15 dBm. The chirp signal from Ant1 is then radiated out toward the target scene.

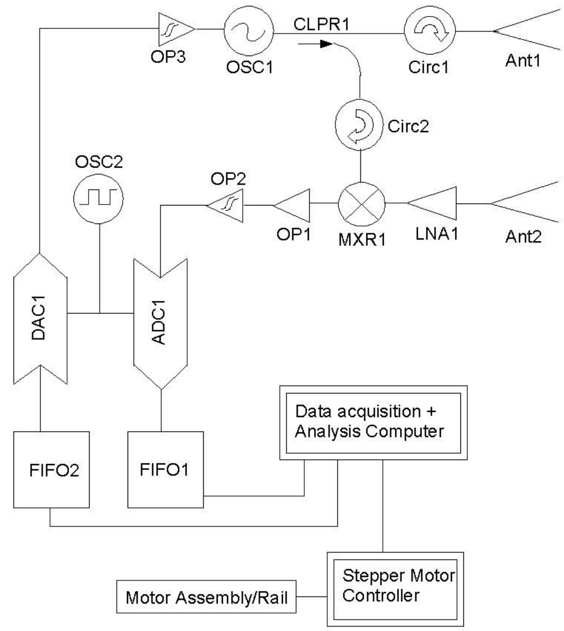

Figure 6: Block diagram of radar system.

Reflected chirp signals from the target scene are then received by the receiver antenna Ant2. Ant2 is a standard gain X-band horn that is fed by a WR90 waveguide transition. The output of Ant2 is fed into LNA1. LNA1 is a 25 dB gain, 8 GHz to 12.4 GHz LNA. The output of LNA1 feeds the RF port of MXR1. The IF output of MXR1 feeds into the video amplifier OP1. The output of OP1 is fed through a 60 KHz active low pass filter OP2. The output of OP2 is the video output of the radar system. This video output contains the beat frequencies which provide range to target information.

The video output of OP2 feeds into the analog to digital converter ADC1. Data acquisition and ramp modulation are performed coherently and synchronized by clock generator OSC2. ADC1 is a 16 bit ADC sampling at 200 KSPS.   ADC1 samples the video output of OP2 coherently with the digital to analog converter DAC1. The output of ADC1 is fed into a first in, first out (fifo) register denoted as FIFO1. The data output of FIFO1 is then transferred to the data acquisition and analysis computer. The data acquisition and analysis computer controls the entire system and its parameters. This computer also processes the range profile data.

The data acquisition and analysis computer fills the second fifo, FIFO2, with values for linear ramp modulation of OSC1. The data from FIFO2 is sampled into DAC1. DAC1 outputs samples coherently with ADC1. The ramp output of DAC1 is a stair cased digital version of a pure ramp. OP3 is a 5 KHz active low pass filter that filters the stair case effect thus smoothing the linear ramp waveform which is modulating OSC1.

The data acquisition and analysis computer also controls the stepper motor controller. The stepper motor controller is connected to an inexpensive biphasic stepper motor. The output shaft of this stepper motor is fed into an old cordless drill planetary gear set transmission in order to multiply the torque up to that required to move the garage door opener rail, see figure 7. The output of the transmission is coupled to the discarded Genie screw type [7] garage door opener rail, see figure 8. A custom machined carrier was made to mount the radar front end onto the garage door opener rail.

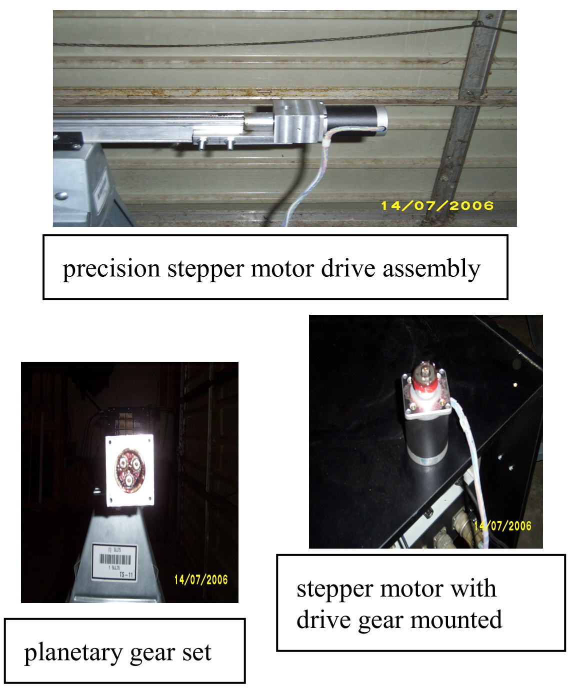

Figure 7: An old cordless drill planetary gear transmission was utilized to multiply the torque from a low cost biphasic stepper motor in order to automatically position the garage door opener based linear rail.

Figure 8: A discarded Genie screw type garage door opener rail was utilized to move the SAR front end.

Utilizing what limited resources were available we were able to successfully implement an FMCW linear rail SAR with large transmit bandwidth and precision positioning capabilities on a budget of only $240 total material cost.

4. Range Profile Data

A number of range profiles were acquired using the low cost high resolution X-band laboratory radar system. These range profiles were acquired to get a rough idea as to the SAR imaging possibilities of this system. Due to the lack of a readily available X-band LNA at the time, these tests were conducted using a chirp bandwidth of only 2.5 GHz rather than the full 4.4 GHz. Radar transmit chirp for these tests spanned 8 GHz to 10.5 GHz. Targets were placed in front of the radar system at various ranges. Range profile data was acquired, converted to complex I and Q in software, and the discrete Fourier Transform was taken to produce the time domain data. Round trip time domain data was converted to linear distance from the radar front end, and shown here. Figure 3 is a picture of the experimental setup, with seven 0 dBsm cylinders placed in the snow (range profile data was acquired outdoors during the winter). Coherent background subtraction was used in all range profile experiments.

Figure 9: Range profile experimental setup showing seven 0 dBsm cylinders spaced every 2 ft placed in the snow.

Figure 10 shows a range profile of seven 0 dBsm cylinders placed in a staggered line spaced every 2 ft, starting at a range of 7 ft and ending at a range of 19 ft. From this range profile plot, the position of each of the seven cylinders is clearly indicated. The first two cylinders are slightly lower in amplitude than the last five. There is a slight range error probably due to slant angle of the radar to the ground. In these experiments, the radar is approximately 2 ft above the line of cylinders. Also, the cylinders are staggered slightly (as shown in Figure 9) so that the maximum amplitude return occurs.

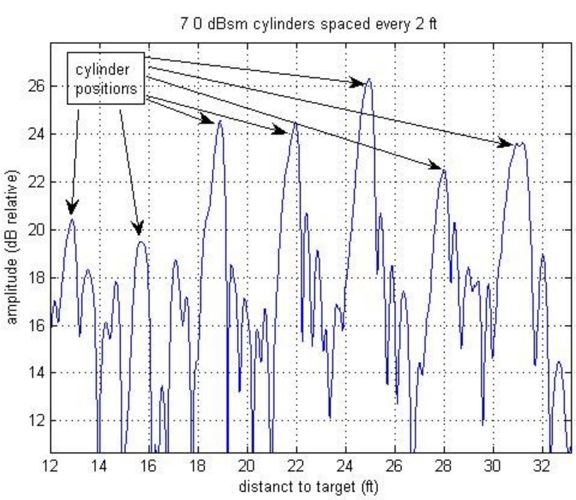

Figure 10: Seven 0 dBsm cylinders spaced every 2 ft.

Figure 11 shows a range profile of seven 0 dB/sm cylinders placed in a staggered line spaced every 1 ft, starting at a range of 7 ft and ending at a range of 13 ft. From this range profile plot, the position of each of the seven cylinders is clearly indicated. There is a slight range error probably due to slant angle of radar and the staggering of cylinders.

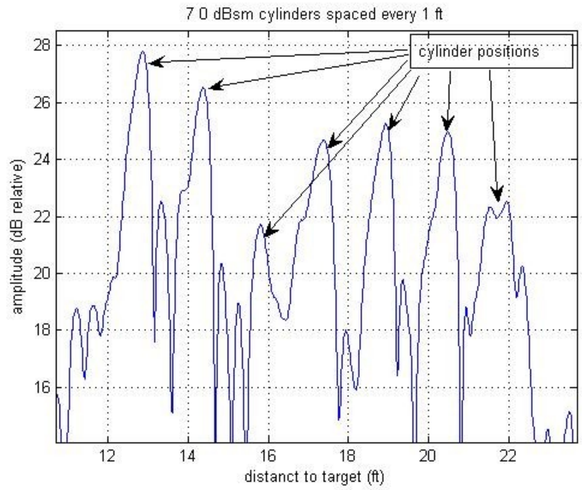

Figure 11: Seven 0 dBsm cylinders spaced every 1 ft.

In both figures 10 and 11 it is clear that the first cylinder at 7ft shows up at approximately 13ft on the radar display. This is due to a constant delay internal to the radar system due physical parts layout and cable lengths. This delay is easily calibrated out later when SAR imagery is made using this system.

5. Synthetic Aperture Radar imagery

SAR imagery was created using 4.4 GHz of chirp bandwidth from 8 GHz to 12.4 GHz. Aperture spacing on the 96 inch linear rail was 0.5 inches per range profile, for a total of 192 range profiles in the data acquisition matrix. The range migration algorithm (RMA) written directly from [6] was utilized as the imaging algorithm.

Radar imagery was created using coherent background subtraction and calibration to an 18 inch tall 3/8 inch diameter aluminum dowel. Figure 12 shows the radar image of a 1:72 scale model B52. Figure 13 shows the radar image of GO STATE written in pushpins. Figure 14 shows the radar image of GO STATE written in 4.37 mm diameter steel spheres.

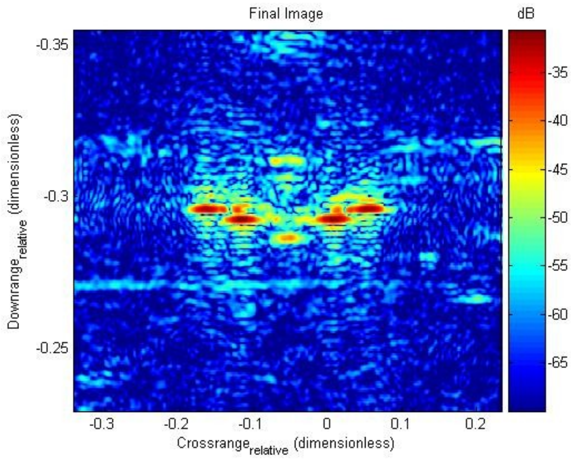

Figure 12: Radar image of a 1:72 scale model B52.

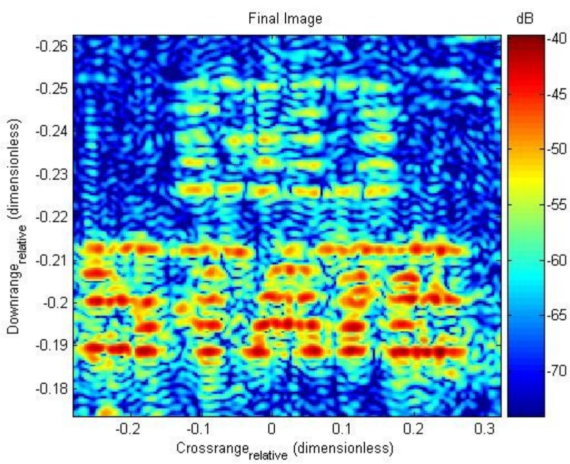

Figure 13: Radar Image of GO STATE made out of pushpins.

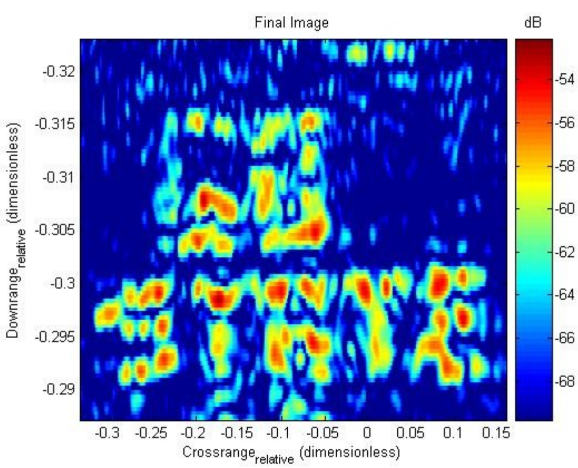

Figure 14: Radar image of GO STATE in 4.37 mm diameter spheres.

From the results shown in figures 12, 13, and 14 it is clear that the low cost, high resolution, X-band linear rail SAR has excellent imaging capabilities, both high resolution and high sensitivity, for a very low cost.

6. Conclusions and Future Work

From the results presented in this paper it is clear that the low cost high resolution X-band laboratory radar system is a capable linear rail SAR imaging system. This system has high resolution capabilities. This was shown in the detailed radar image a 1:72 scale model of a B52. This system is also sensitive, shown capable of imaging small targets such as pushpins and 4.37 mm steel spheres. Innovations such as utilizing a discarded garage door opener and a transmission from an old cordless drill allowed the MSU Electromagnetics Group to develop a rail SAR on the budget of approximately $240. Potential future work on this project will include studies on advanced motion compensation and Autofocus techniques.

7. REFERENCES

[1] M. P. G. Capelli, "Radio Altimeter," IRE Transactions on Aeronautical and Navigational Electronics, vol. 1, pp. 3-7; June 1954.

[2] M. I. Skolnic, *Radar Handbook*. New York: McGraw-Hill, 1970.

[3] G. L. Charvat, L. C. Kempel. "Synthetic Aperture Radar Imaging Using a Unique Approach to Frequency-Modulated Continuous-Wave Radar Design." IEEE Antennas and Propagation Magazine, February 2006.

[4] G. L. Charvat, "A Unique Approach to Frequency-Modulated Continuous-Wave Radar Design." East Lansing MI: A thesis, submitted to Michigan State University, 2003, in partial fulfillment of the requirements for the degree of Master of Science.

[5] G. L. Charvat, L. C. Kempel. "Low-Cost, High Resolution X-Band Laboratory Radar System for Synthetic Aperture Radar Applications." East Lansing, MI: IEEE Electro/Information Technology Conference, May 2006.

[6] W. G. Carrara, R. S. Goodman, R. M. Majewski, *Spotlight Synthetic Aperture Radar Signal Processing Algorithms.* Boston: Artech House, 1995.

[7] http://www.geniecompany.com/